SUPPORTING INFORMATION FOR

Selective complexation of divalent cations by a cyclic α,β-peptoid hexamer: a spectroscopic and computational study.

E. De Santis,[*a]† A. A. Edwards,[a] B. D. Alexander,[b] S. J. Holder,[*c] A.-S. Biesse-Martin,[d,] B. V. Nielsen,[b] D. Mistry,[e] L. Waters,[e] G. Siligardi,[f] R. Hussain,[f] S. Faure[d] and C. Taillefumier[*d]

[a]*Medway School of Pharmacy, Universities of Kent and Greenwich at Medway, Central Avenue, Chatham Maritime, Kent ME4 4TB, UK;*
[b]*School of Science, University of Greenwich, Central Avenue, Chatham Maritime, Kent ME4 4TB, UK;*
[c]*Functional materials Group, School of Physical Sciences, University of Kent, Canterbury, CN2 7NZ, UK;*
[d]*Université Clermont Auvergne, Université Blaise Pascal, Institut de Chimie de Clermont-Ferrand, BP 10448, F-63000 Clermont-Ferrand, France and CNRS, UMR 6296, ICCF, F-63178 Aubière Cedex, France.*
[e]*Division of Pharmacy and Pharmaceutical Sciences, University of Huddersfield, Queensgate, Huddersfield, UK;*
[f]*Diamond Light Source Ltd., Diamond House, Harwell Science and Innovation Campus, Didcot, Oxfordshire, OX11 0DE, UK.*
†Current address: National Physical laboratory, Hampton road, Teddington, Middlesex, TW11 0LW, UK.

TABLE OF CONTENTS

1) HPLC and NMR spectra of cP1

Copy of analytical HPLC analysis of cyclic α,β-peptoid cP1
Conditions: Solvent A: water (0.1% TFA); solvent B: MeCN; solvent C: MeOH; A/B 20:80, flow = 0.80; 214 nm.

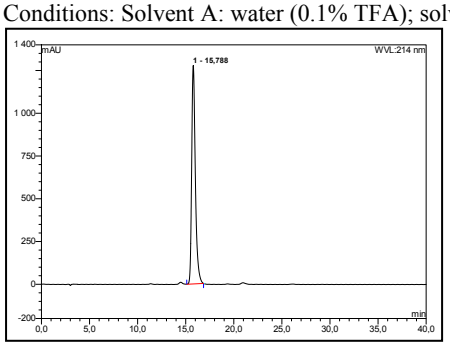

Copy of NMR spectra of cyclic α,β-peptoid cP1 (acetone-d_6)

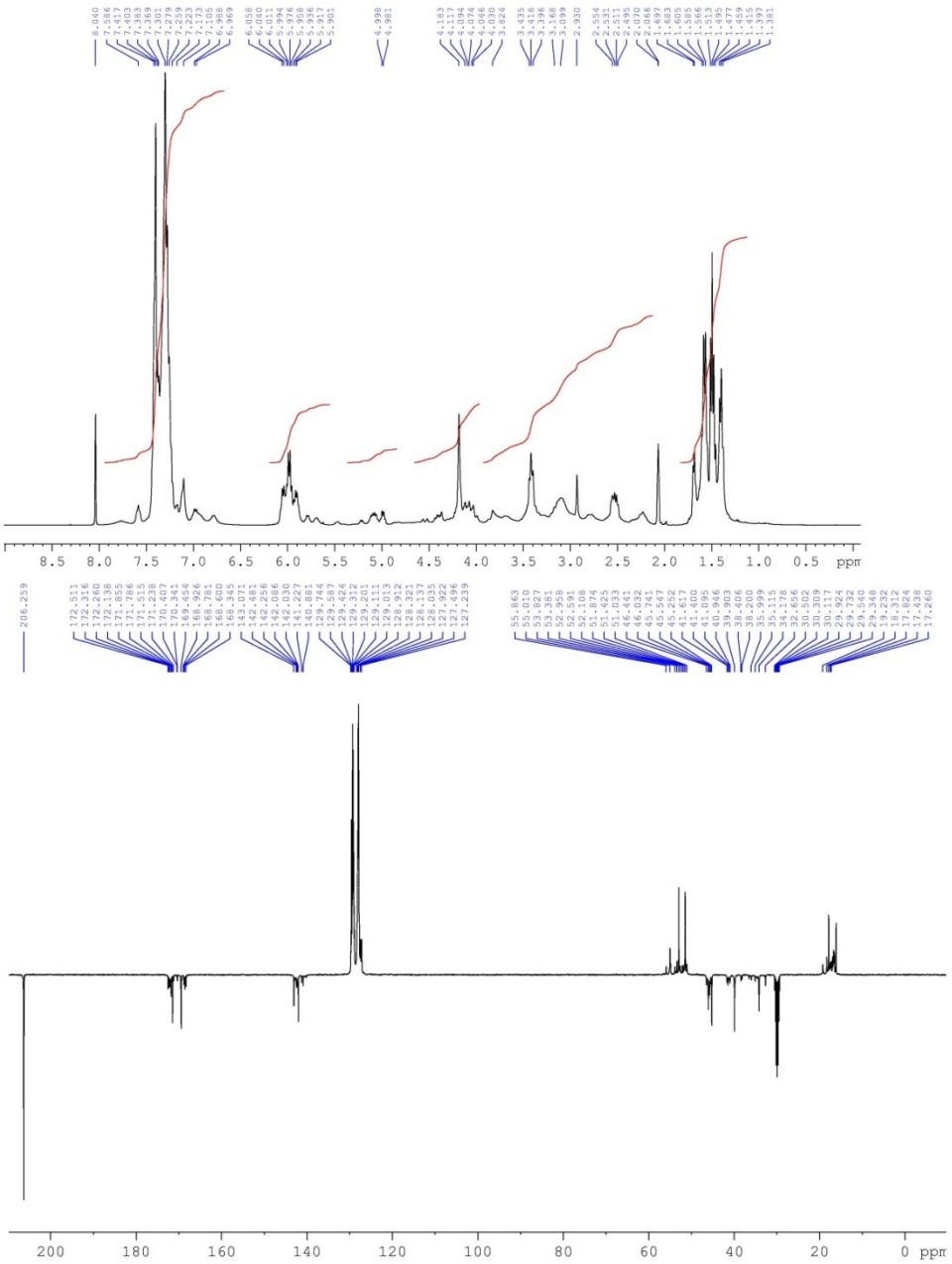

2) Complexation study by NMR

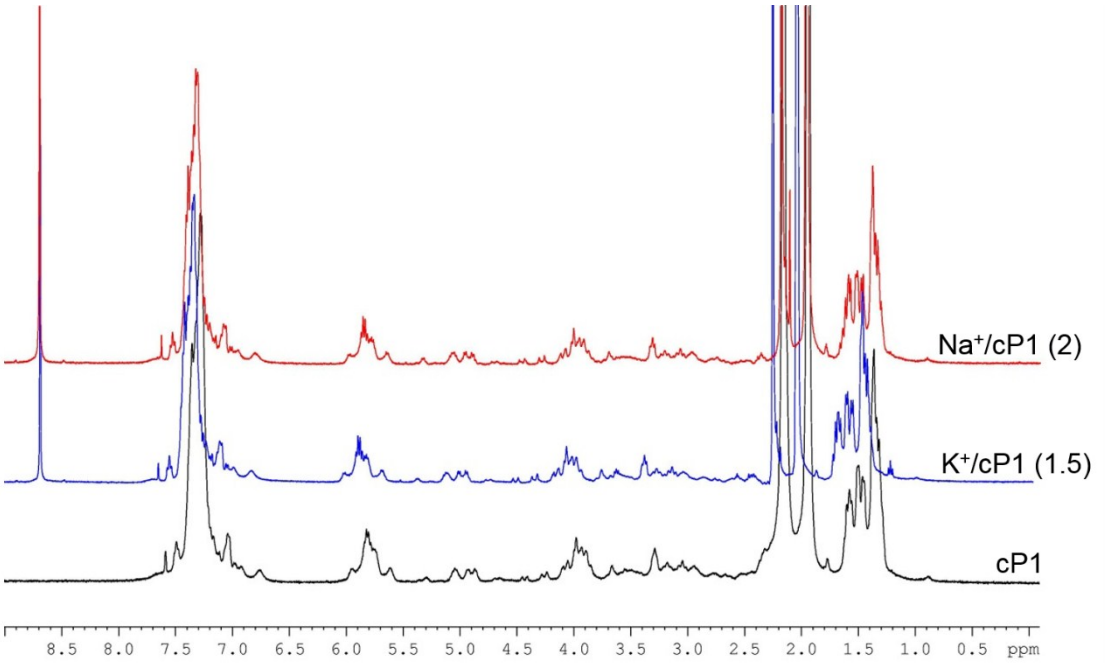

Fig. S1 ^{1}H NMR spectra in CD_3CN of cyclopeptoid **cP1** alone and in the presence of picrate salts of sodium and potassium in the molar ratio (metal/peptoid) indicated in brackets. Spectra were recorded at 20 °C using a peptoid concentration of 4 mM.

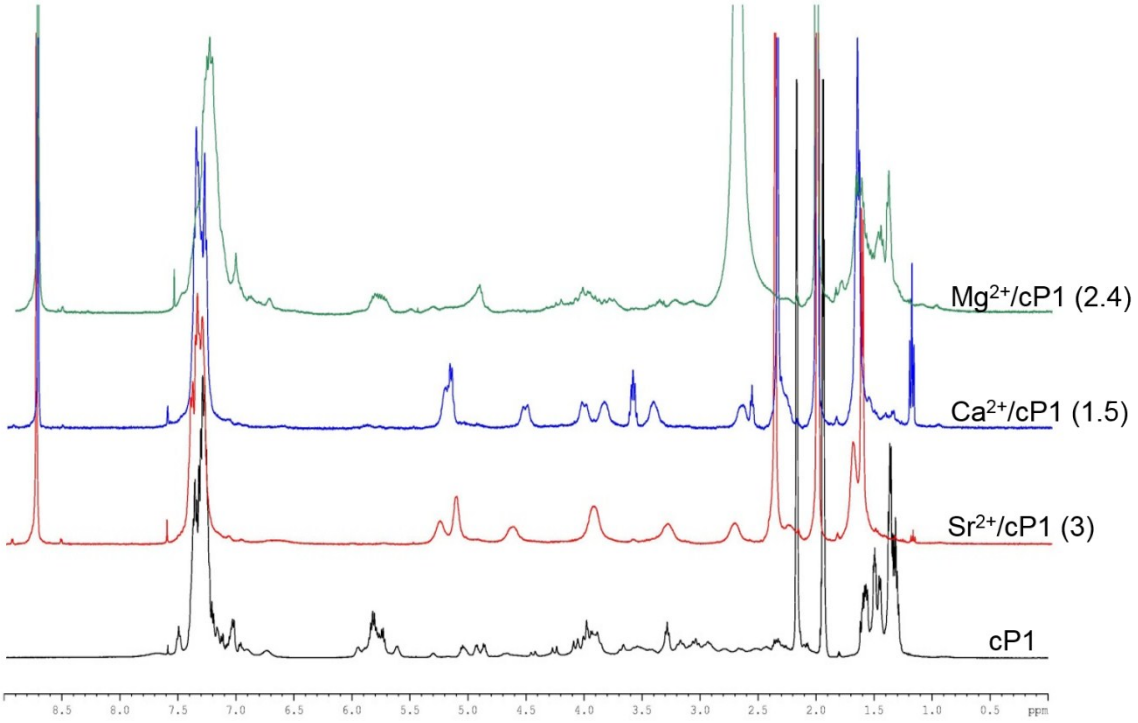

Fig. S2 ^{1}H NMR spectra in CD_3CN of cyclopeptoid **cP1** alone and in the presence of picrate salts of strontium, calcium and magnesium in the molar ratio (metal/peptoid) indicated in brackets. Spectra were recorded at 20 °C using a peptoid concentration of 4 mM.

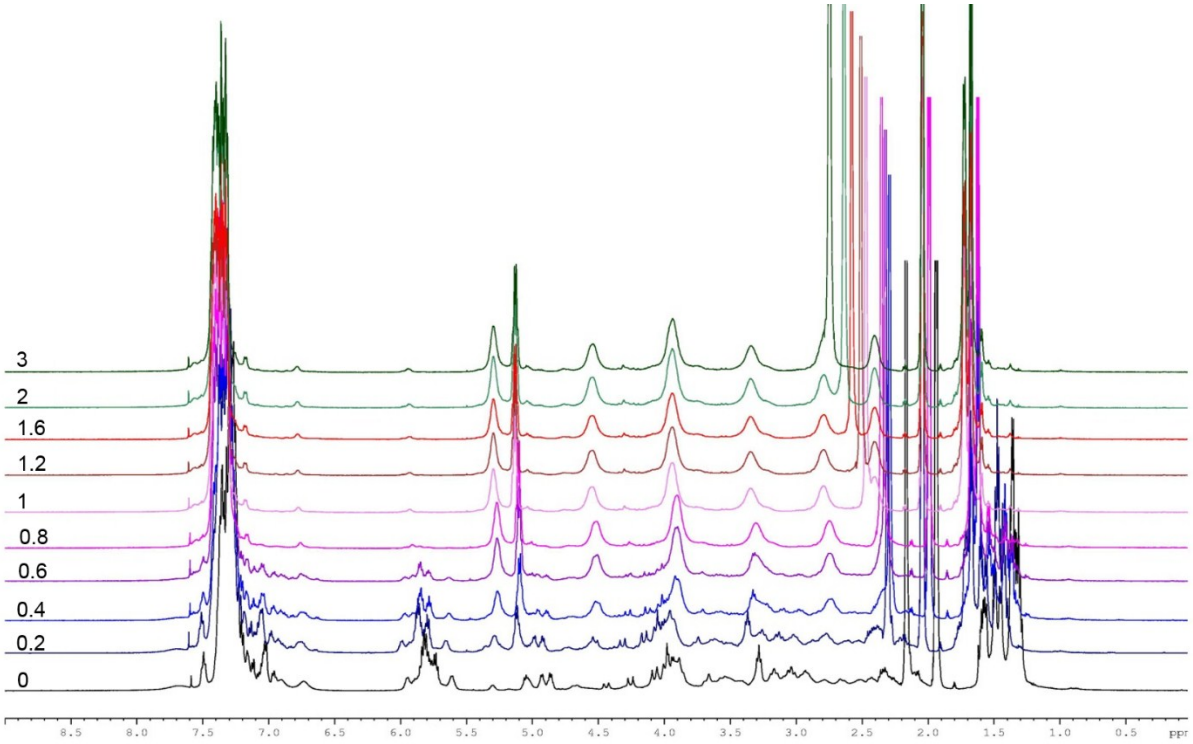

Fig. S3 Quantitative titration by ^{1}H NMR of $Sr(ClO_4)_2.6H_2O$ into peptoid **cP1** at the molar ratios (Sr^{2+}/**cP1**) indicated. All experiments were performed in CD_3CN at 293K using a peptoid concentration of 8 mM.

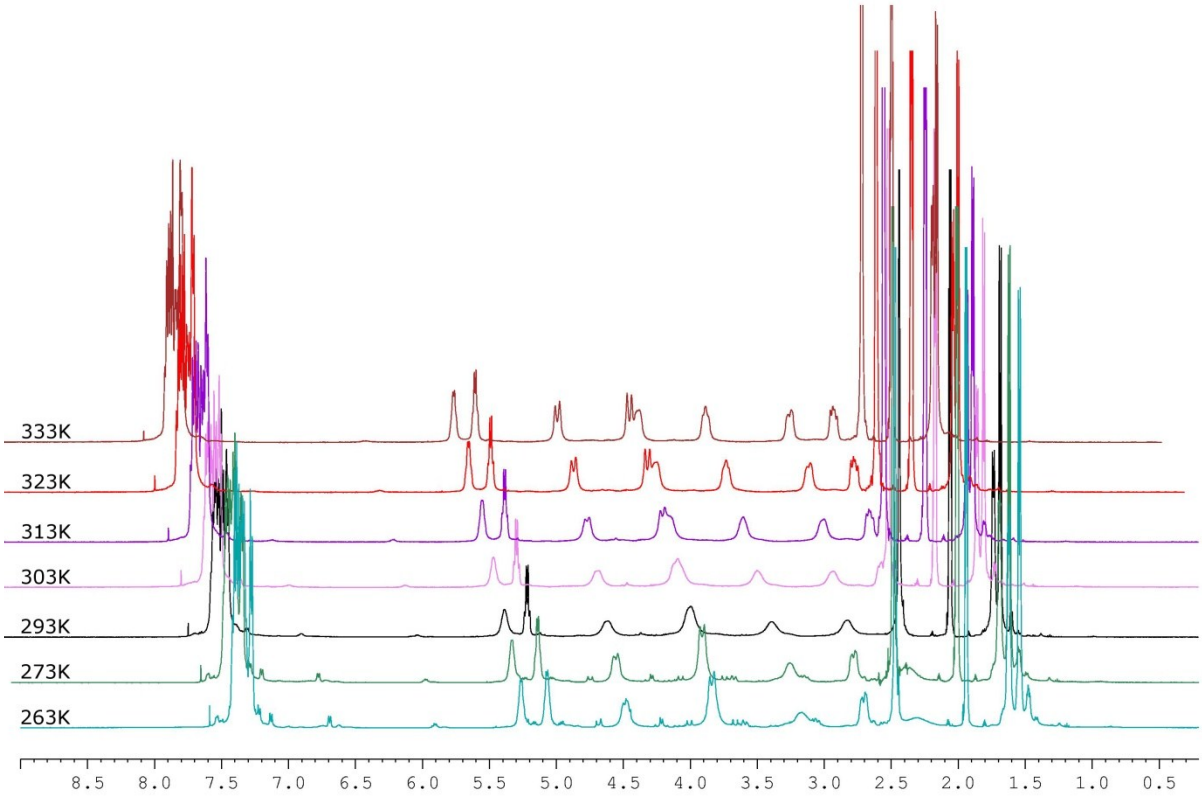

Fig. S4 ^{1}H NMR temperature study on a 1:1 mixture of peptoid **cP1** and $Sr(ClO_4)_2.6H_2O$ at a concentration of 8 mM in CD_3CN.

NMR spectra of Sr^{2+}/cP1 complex:

^{1}H NMR spectra of Sr^{2+}/**cP1** complex (CD_3CN, 293K)

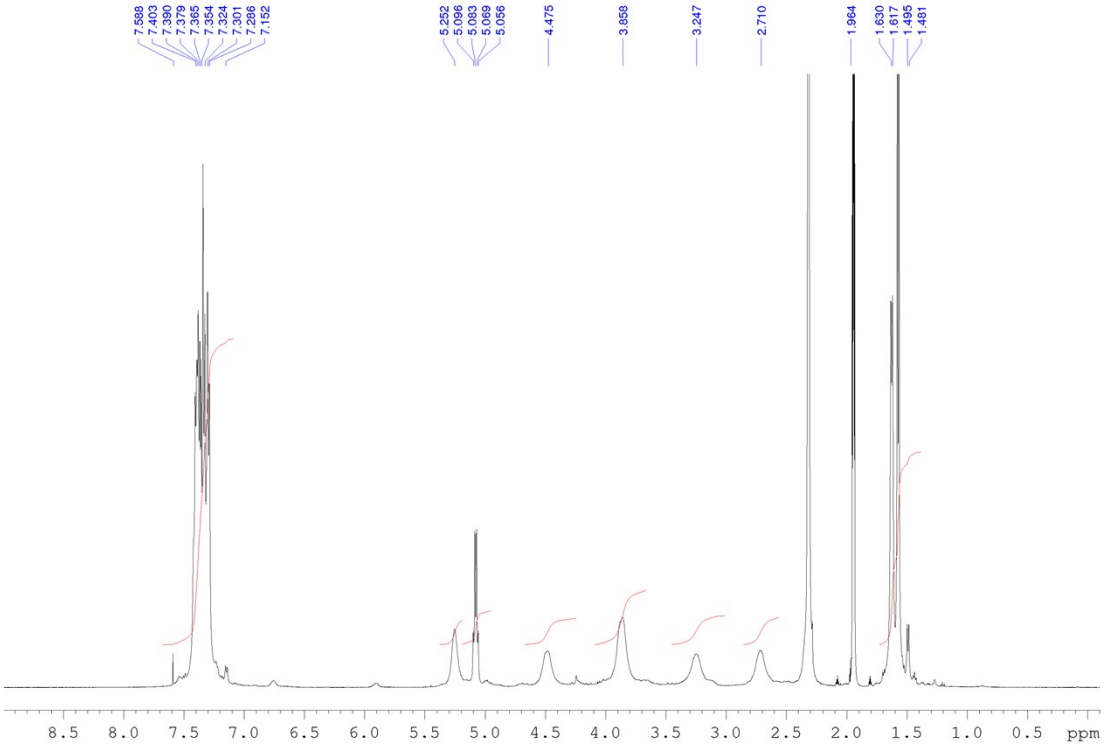

^{13}C NMR spectra of Sr^{2+}/**cP1** complex (CD_3CN, 293K)

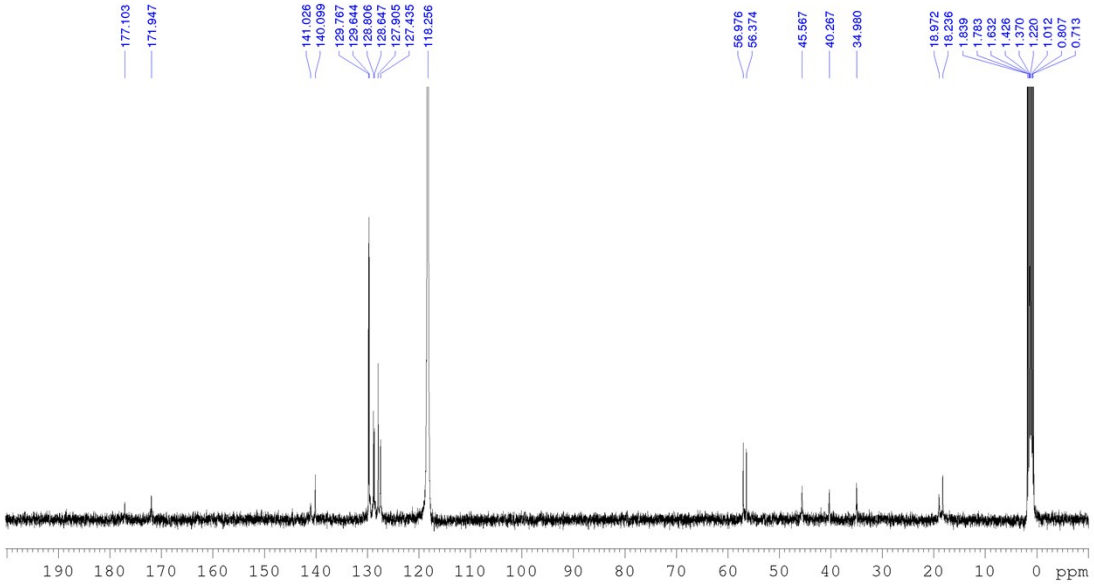

Table S1 Proton and carbon chemical shifts for metal complex (Sr^{2+}/**cP1**, 1) in CD_3CN at 333K.

proton	^{1}H chemical shift (ppm)	signal	Coupling constant (Hz)	^{13}C chemical shift (ppm)
H^7	1.60	d	*J* 7	18.2
H^9	1.63	d	*J* 6.5	18.8
H^2, $H^{2'}$	2.38, 2.70	dd, m (AB syst)	J_{AB} 15.5 *J* 9	34.6
H^3, $H^{3'}$	3.34, 3.84	m, m (AB syst)		40.0
H^5, $H^{5'}$	3.93, 4.45	d, d (AB syst)	J_{AB} 16.5	45.2
H^6	5.08	q	7	56.1
H^8	5.25	q	6.5	56.6
H Ph	7.27-7.44	m		

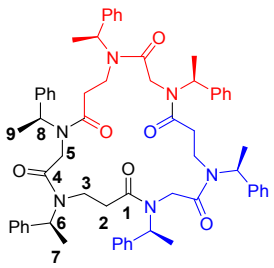

^{1}H NMR spectra of Sr^{2+}/**cP1** complex (CD_3CN, 333K)

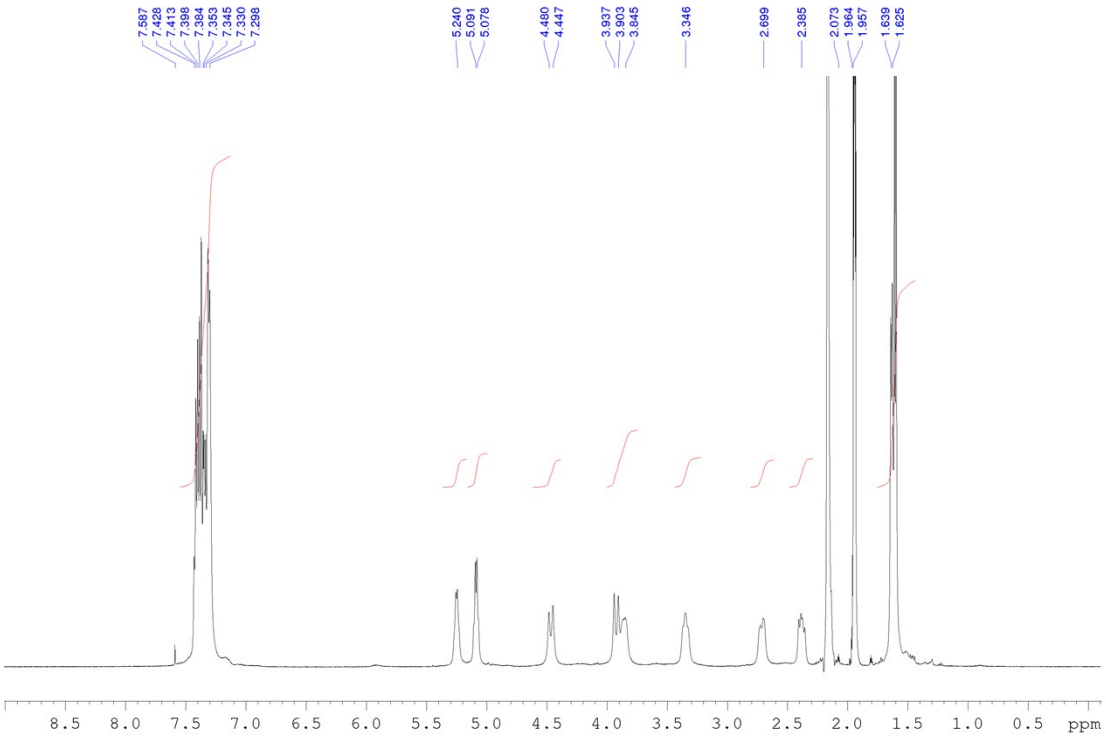

^{1}H NMR spectra of Ca^{2+}/cP1 complex (CD_3CN, 293K):

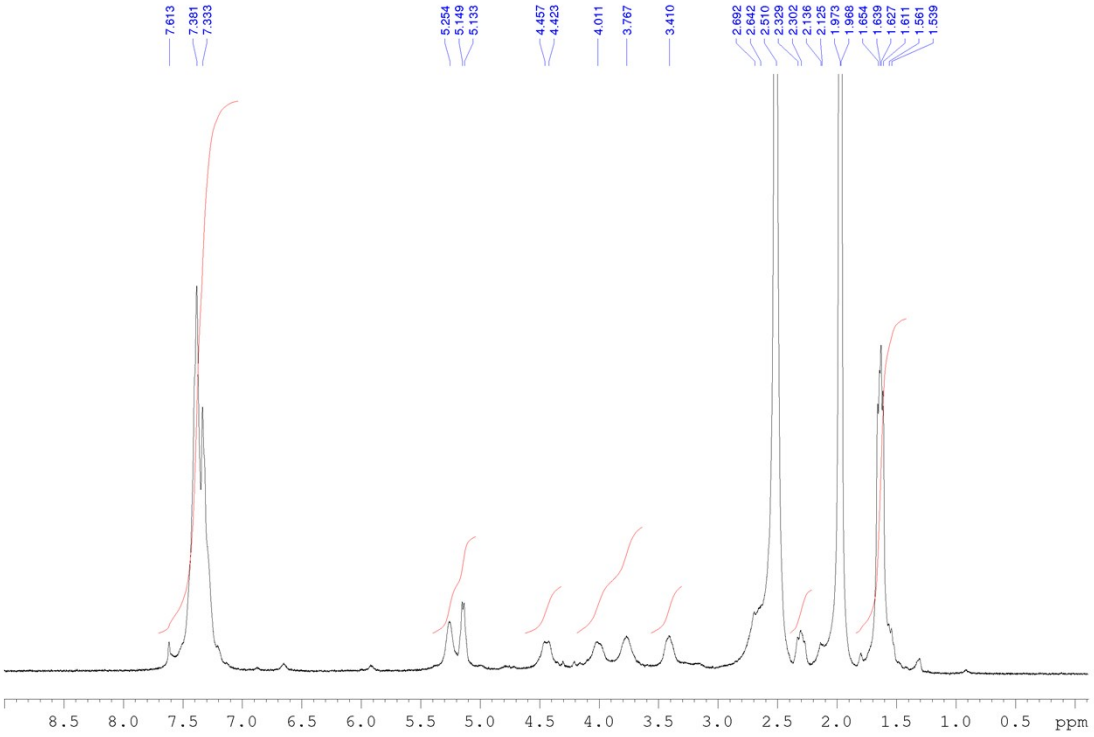

3) Complexation study by circular dichroism

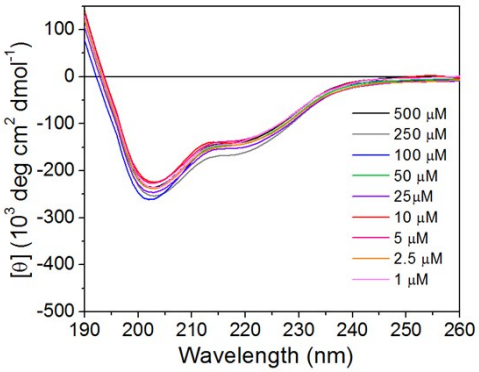

Fig. S5 Concentration study of peptoid **cP1** in CH_3CN by ECD. All spectra were recorded at 20 °C at the concentrations stated using cells of pathlengths: 0.01 cm (500 – 100 µM), 0.1 cm (50 – 10 µM) or 1 cm (5 – 1 µM).

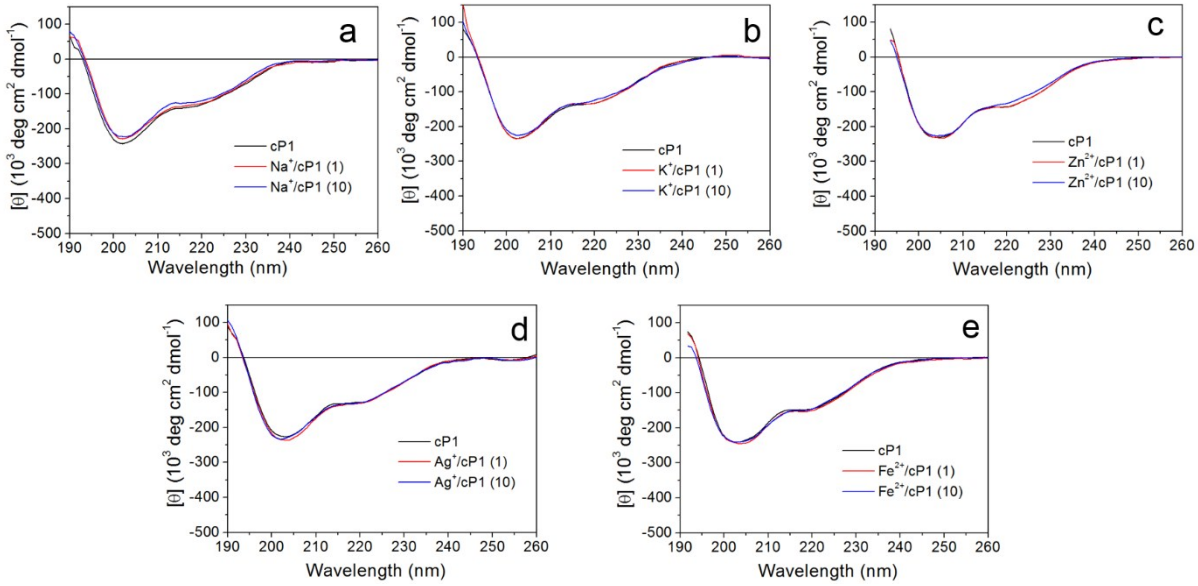

Fig. S6. Qualitative titration by SRCD of **cP1** with the perchlorate salts of (a) sodium, (b) potassium, (c) zinc, (d) silver and (e) iron(II) at the molar ratio (metal/peptoid) indicated in brackets. All spectra were recorded in CH_3CN at 20 °C with a peptoid concentration of 7.5 µM and a 0.4 cm pathlength cell for sodium, potassium and silver and with 15 µM **cP1** concentration and 1.0 cm pathlength cell for zinc and iron(II).

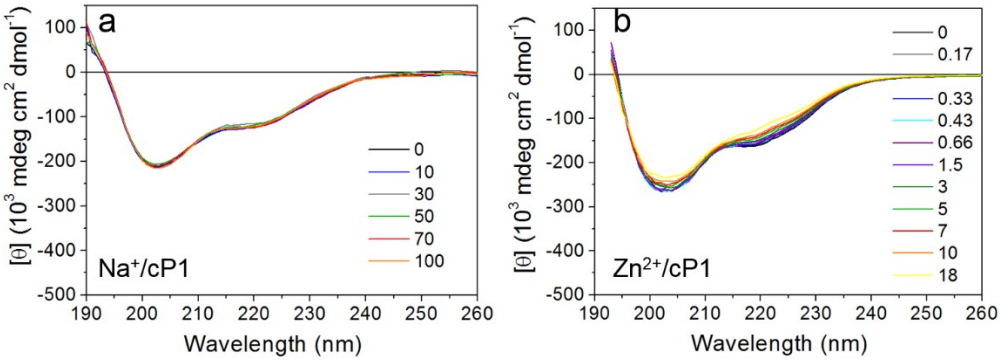

Fig. S7 Quantitative titration by SRCD of **cP1** with perchlorate salts of (a) sodium and (b) zinc. Spectra recorded at 20 °C with a peptoid concentration of 7.5 µM and indicate molar ratio using a 0.4 cm pathlength cell.

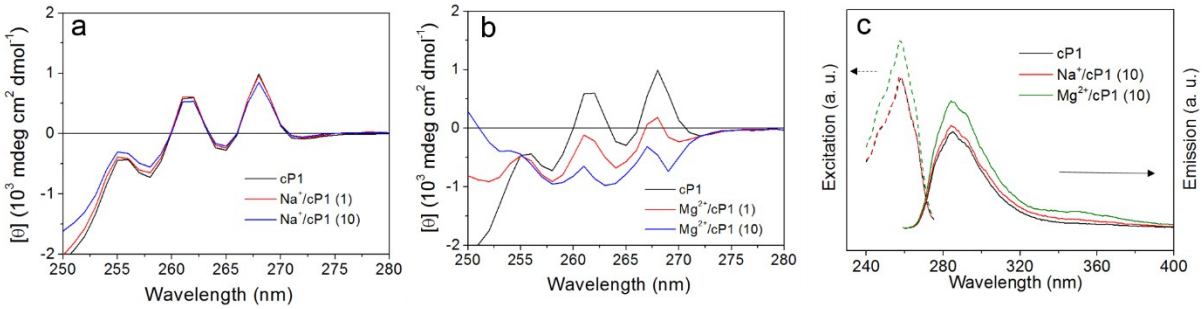

Fig. S8. Complexation experiments by multiple spectroscopic techniques in CH_3CN. Qualitative titration by ECD of **cP1** in the near UV region with (a) $Na(ClO_4)$ and (b) $Mg(ClO_4)_2$. (c) Fluorescence spectra of **cP1**, Na^+/**cP1** and Mg^{2+}/**cP1** complex. CD and fluorescence spectra were recorded at 20 °C with a peptoid concentration of 600 μM using a 1 cm pathlength cell. For fluorescence spectra excitation (dashed line) was set at 250 nm and emission (solid line) at 284 nm.

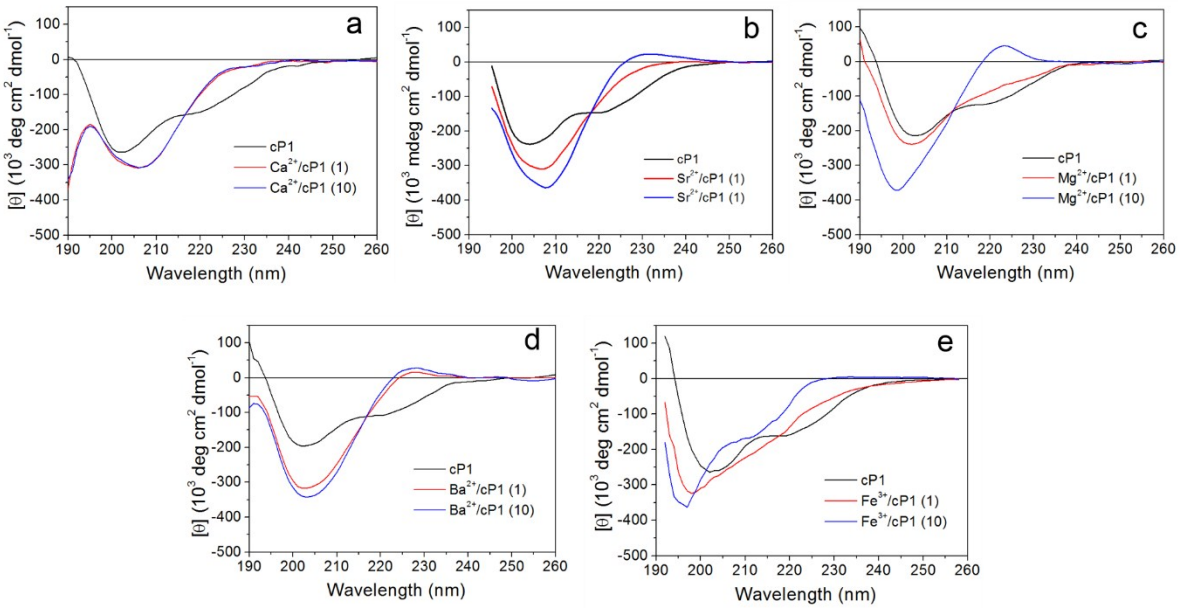

Fig. S9 Qualitative titration by SRCD of **cP1** with the perchlorate salts of (a) calcium, (b) strontium, (c) magnesium, (d) barium and (e) iron(III) at the molar ratio (metal/peptoid) indicated in brackets. All spectra were recorded in CH_3CN at 20 °C with a peptoid concentration of 7.5 μM and a 0.4 cm pathlength cell for calcium, magnesium and barium and with 15 μM **cP1** concentration and 1.0 cm pathlength cell for strontium and iron(III).

4) Modelling of metal complexes

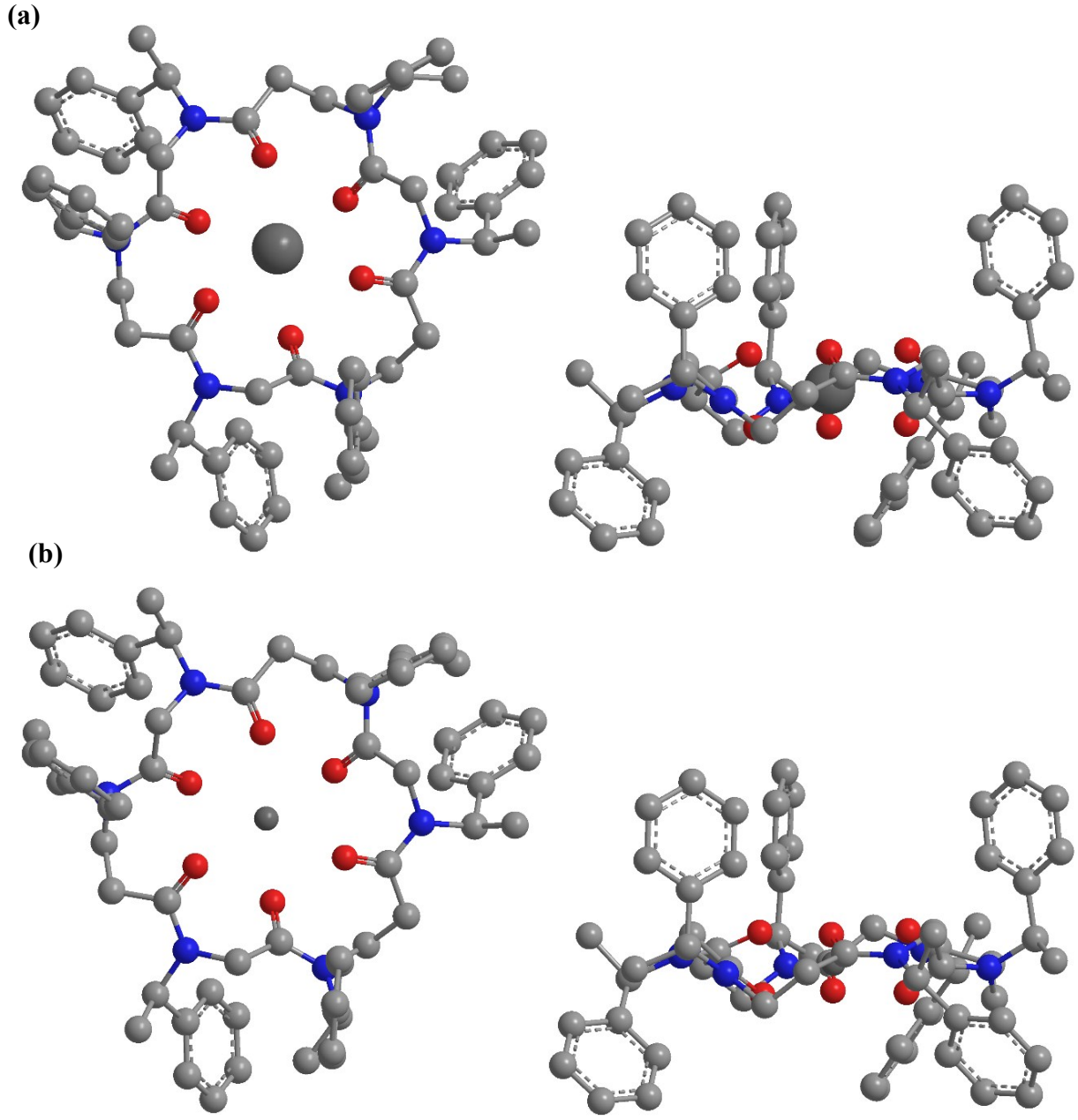

Fig. S10
(a) Top and side view of 6-coordinate Sr^{2+}/**cP1** complex (PM6). (b) Top and side view of 6-coordinate Ca^{2+}/**cP1** complex (PM6). Hydrogens are omitted for clarity in both cases. The relatively smaller size of the Ca^{2+} ion compared to that of the Sr^{2+} ion is due to the atoms being represented in Chem3D by their VdW radii rather than ionic and does not reflect the ion size used in the PM6 modelling.

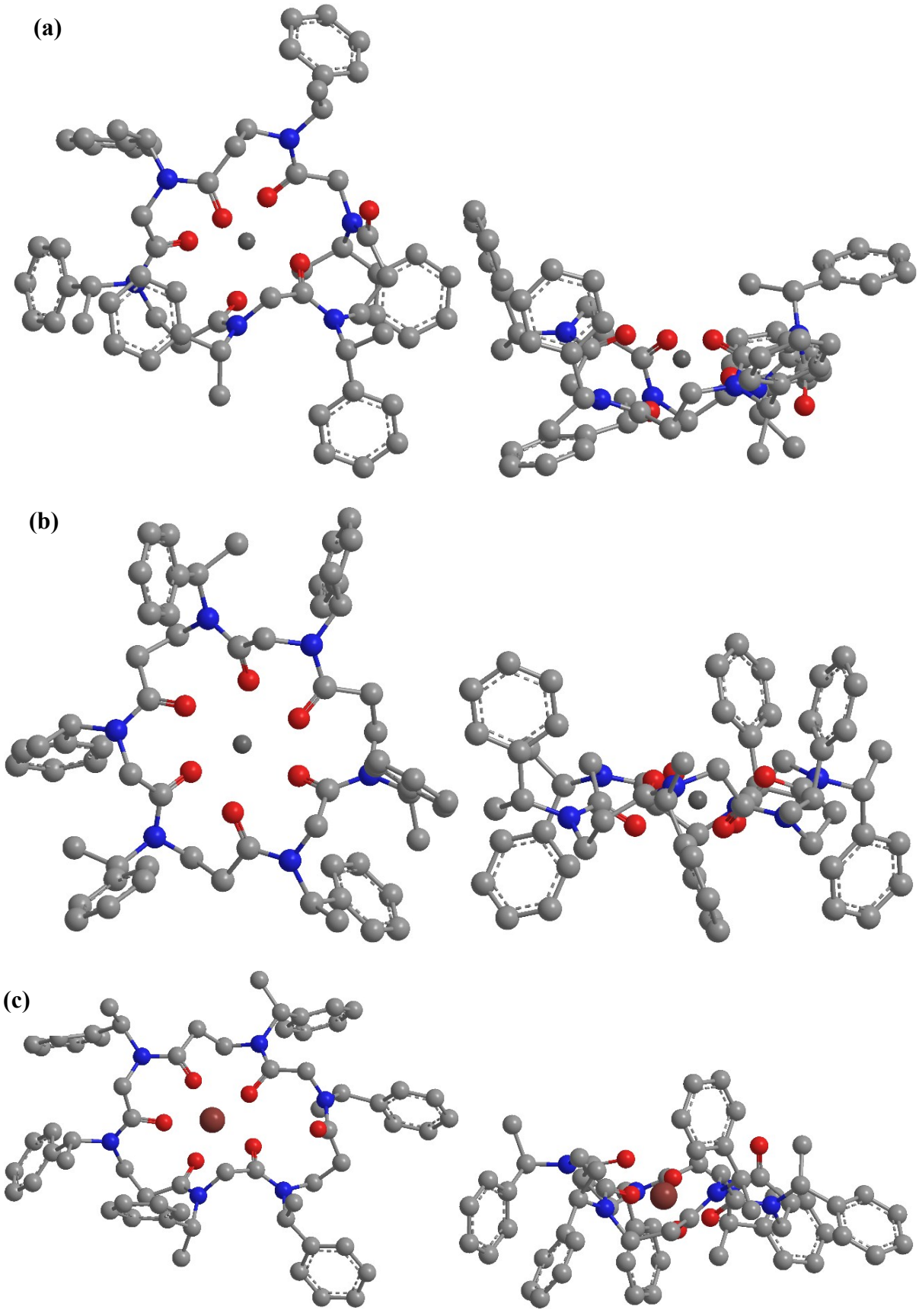
(a)
(b)
(c)

(d)

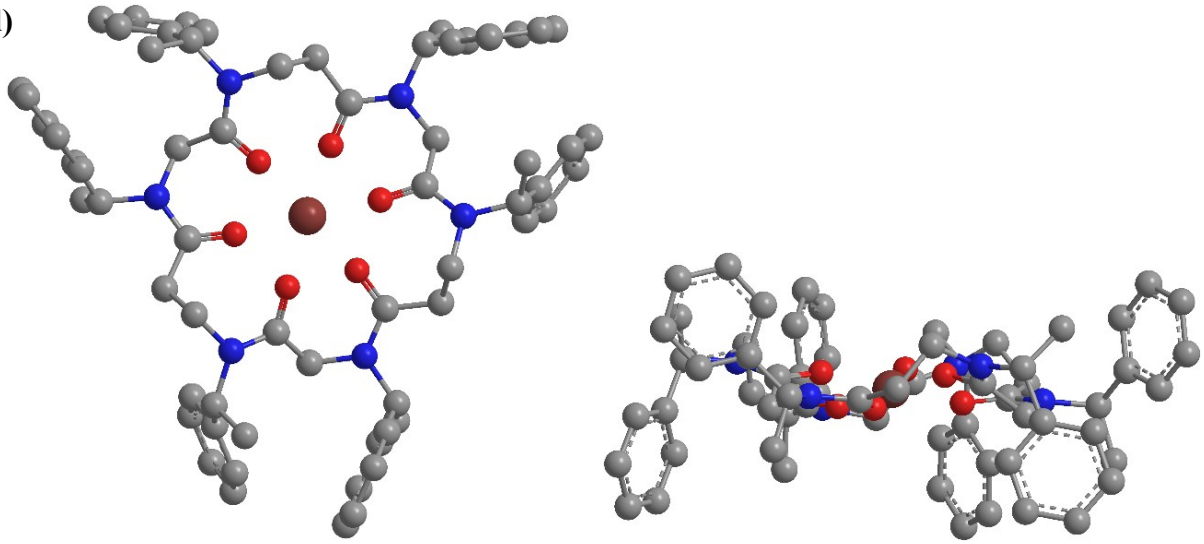

Fig. S11 (a) Top and side view of 5-coordinate Mg^{2+}/**cP1** complex (PM6). (b) Top and side view of high energy 6 coordinate Mg^{2+}/**cP1** complex (PM6). (c) Top and side view of 5 coordinate Fe^{3+}/**cP1** complex (PM6). (d) Top and side view of high energy 6 coordinate Fe^{3+}/**cP1** complex (PM6).

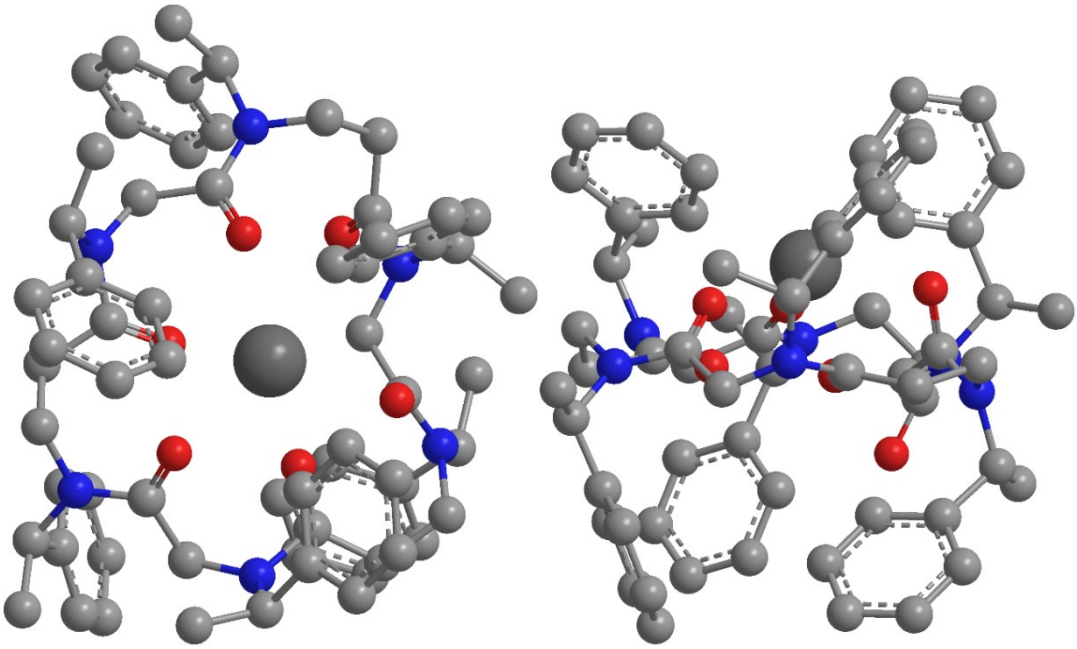

Fig. S12 Top and side view of 6-coordinate Ba^{2+}/**cP1** complex (PM6). Hydrogens omitted for clarity.

Table S2: Heats of formation and total energies of conformers as calculated by PM6 using a COSMO solvation model for acetonitrile.

	6-cordinate conformer		**5-coordinate conformer**	
M/cP1 complex	**ΔH_f (kJ mol^{-1})**	**Total energy (eV)**	**ΔH_f (kJ mol^{-1})**	**Total energy (eV)**
Sr^{2+}	-259.0	-11534.88847	-	-
Ca^{2+}	-274.7	-11534.60230	-	-
Ba^{2+}	-1228.6	-11543.88515	-	-
Mg^{2+}	-105.2	-11538.91321	-141.0	-11539.27676
Fe^{3+}	520.2	-11940.00922	565.5	-11939.55470

5) Quantification of the binding by circular dichroism

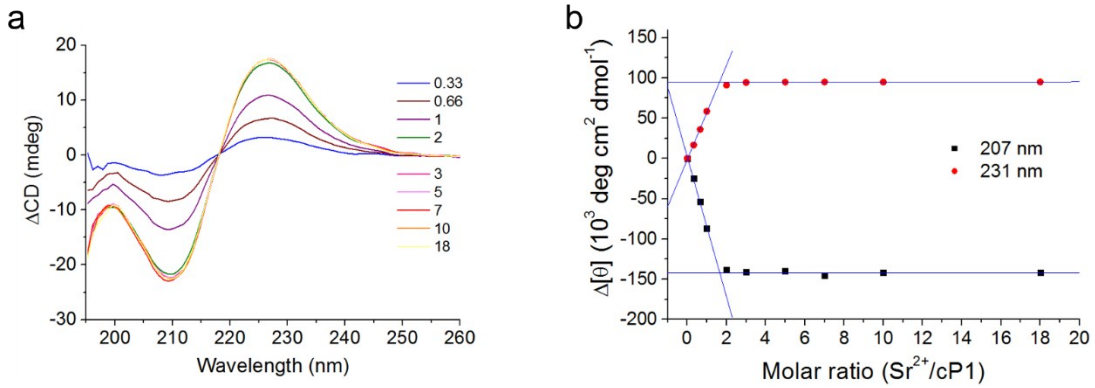

Fig. S13 Quantitative titration of $Sr(ClO_4)_2$ into the cyclopeptoid **cP1**. (a) Differential SRCD spectra of Sr^{2+}/**cP1** complexes at the molar ratio indicated and (b) a plot of the differential molar ellipticity versus the molar ratio (Sr^{2+}/**cP1**) at the wavelengths indicated. All CD spectra were recorded in CH_3CN at 20 °C with a **cP1** concentration of 15 µM using a 1 cm pathlength cell.

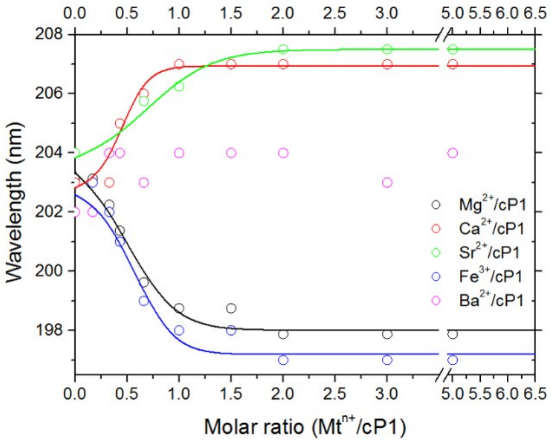

Fig. S14 Wavelength shifts for the maximum below 210 nm for all titrations.

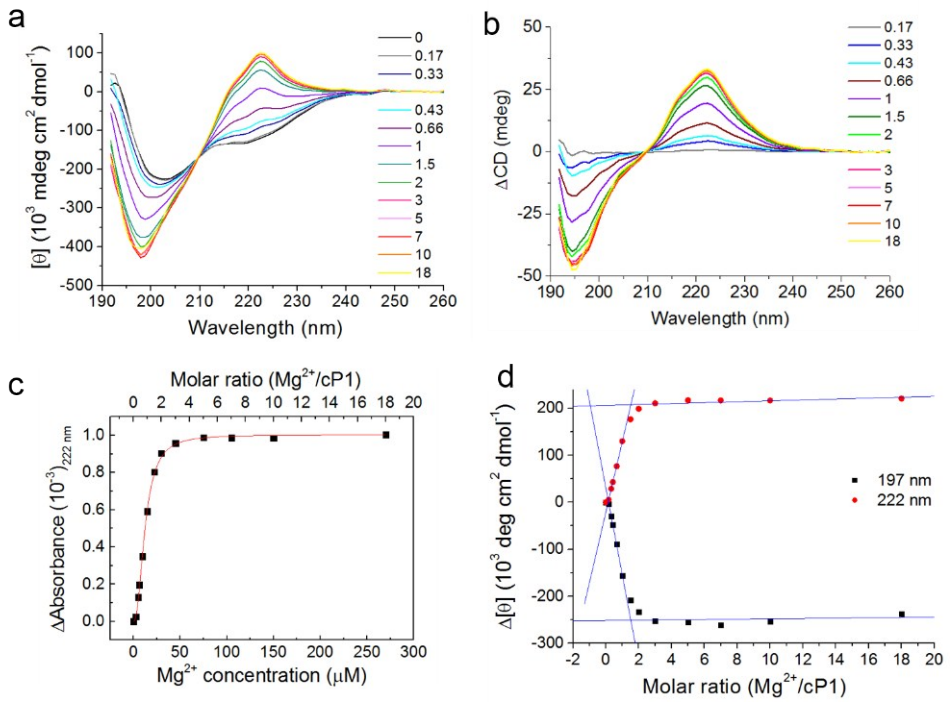

Fig. S15 Quantitative titration of $Mg(ClO_4)_2$ into **cP1** by SRCD in CH_3CN. (a) Molar ellipticity spectra of **cP1** upon titration with different molar ratios of $Mg(ClO_4)_2$ as indicated. (b) Differential CD spectra of Mg^{2+}/**cP1** complexes at the molar ratio indicated. (c) A plot of the ΔA at 222 nm as a function of the concentration of Mg^{2+} and molar ratio with fitting to the Hill equation (K_d = 12 ± 0.2 μM, R^2 = 0.99). (d)) A plot of the differential molar ellipticity versus the molar ratio (Mg^{2+}/**cP1**) at the wavelengths indicated. All spectra were recorded at 20 °C at a peptoid concentration of 15 μM using a 1 cm pathlength cell.

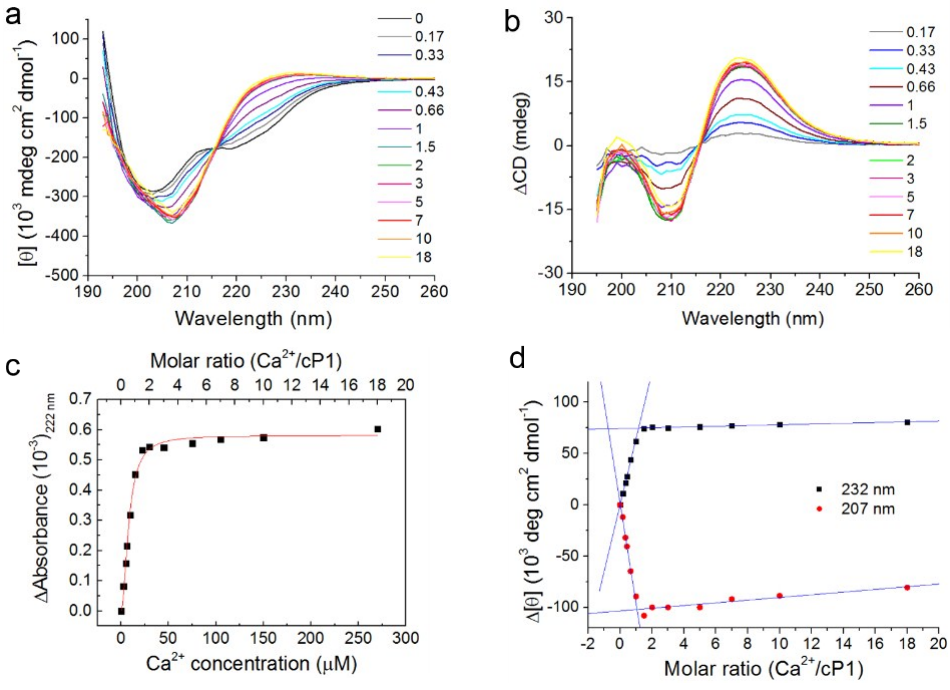

Fig. S16 Quantitative titration of $Ca(ClO_4)_2$ into **cP1** by SRCD in CH_3CN. (a) Molar ellipticity spectra of **cP1** upon titration with different molar ratios of $Ca(ClO_4)_2$ as indicated. (b) Differential CD spectra of Ca^{2+}/**cP1** complexes at the molar ratio indicated. (c) A plot of the ΔA at 222 nm as a function of the concentration of Ca^{2+} and molar ratio with fitting to the Hill equation (Kd = 8.2 ± 0.35 μM, R^2 = 0.99). (d)) A plot of the differential molar ellipticity versus the molar ratio (Ca^{2+}/**cP1**) at the wavelengths indicated. All spectra were recorded at 20 °C at a peptoid concentration of 15 μM using a 1 cm pathlength cell.

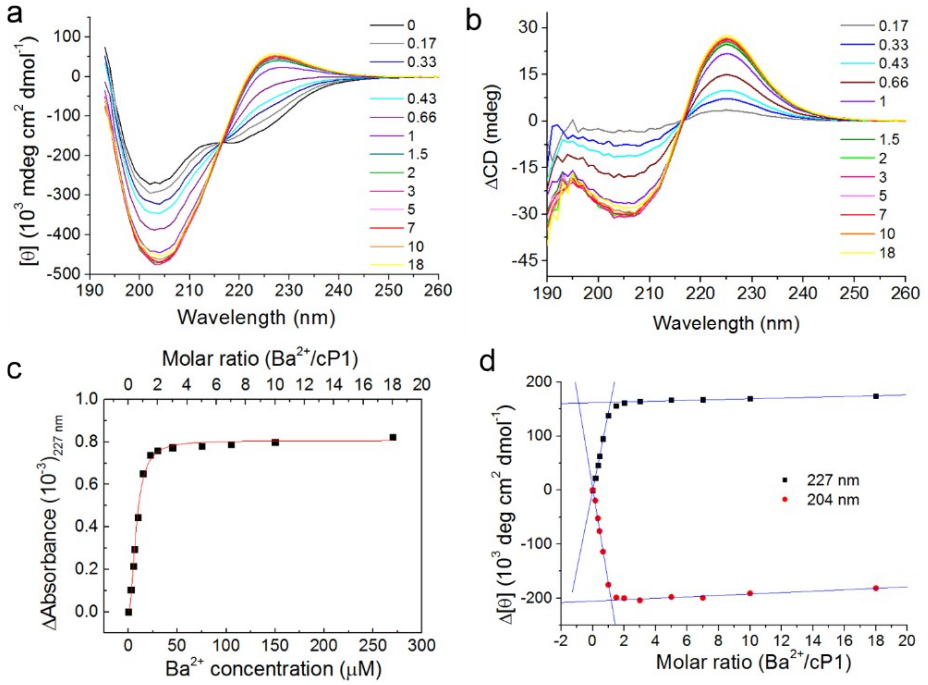

Fig. S17 Quantitative titration of $Ba(ClO_4)_2$ into **cP1** by SRCD in CH_3CN. (a) Molar ellipticity spectra of **cP1** upon titration with different molar ratios of $Ba(ClO_4)_2$ as indicated. (b) Differential CD spectra of Ba^{2+}/**cP1** complexes at the molar ratio indicated. (c) A plot of the ΔA at 227 nm as a function of the concentration of Ba^{2+} and molar ratio with fitting to the Hill equation (Kd = 8.2 ± 0.28 μM, R^2 = 0.99). (d)) A plot of the differential molar ellipticity versus the molar ratio (Ba^{2+}/**cP1**) at the wavelengths indicated. All spectra were recorded at 20 °C at a peptoid concentration of 15 μM using a 1 cm pathlength cell.

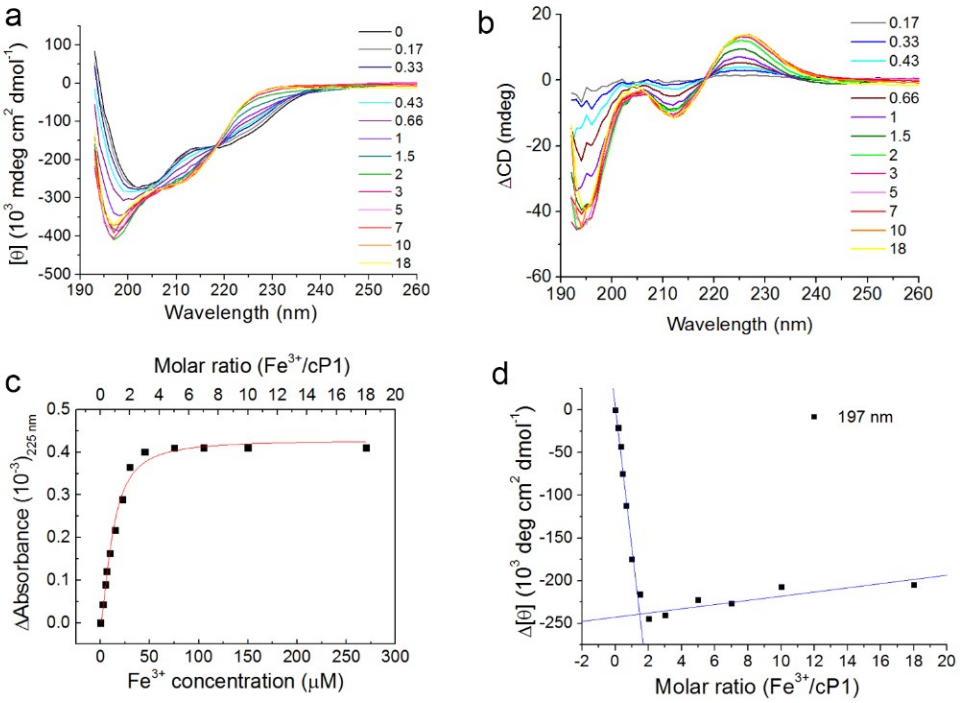

Fig. S18 Quantitative titration of $Fe(ClO_4)_3$ into **cP1** by SRCD in CH_3CN. (a) Molar ellipticity spectra of **cP1** upon titration with different molar ratios of $Fe(ClO_4)_3$ as indicated. (b) Differential CD spectra of Fe^{3+}/**cP1** complexes at the molar ratio indicated. (c) A plot of the ΔA at 225 nm as a function of the concentration of Fe^{3+} and molar ratio with fitting to the Hill equation (Kd = 12,7 ± 0.86 μM, R^2 = 0.99). (d)) A plot of the differential molar ellipticity versus the molar ratio (Fe^{3+}/**cP1**) at the wavelengths indicated. All spectra were recorded at 20 °C at a peptoid concentration of 15 μM using a 1 cm pathlength cell.

6) Additional figure

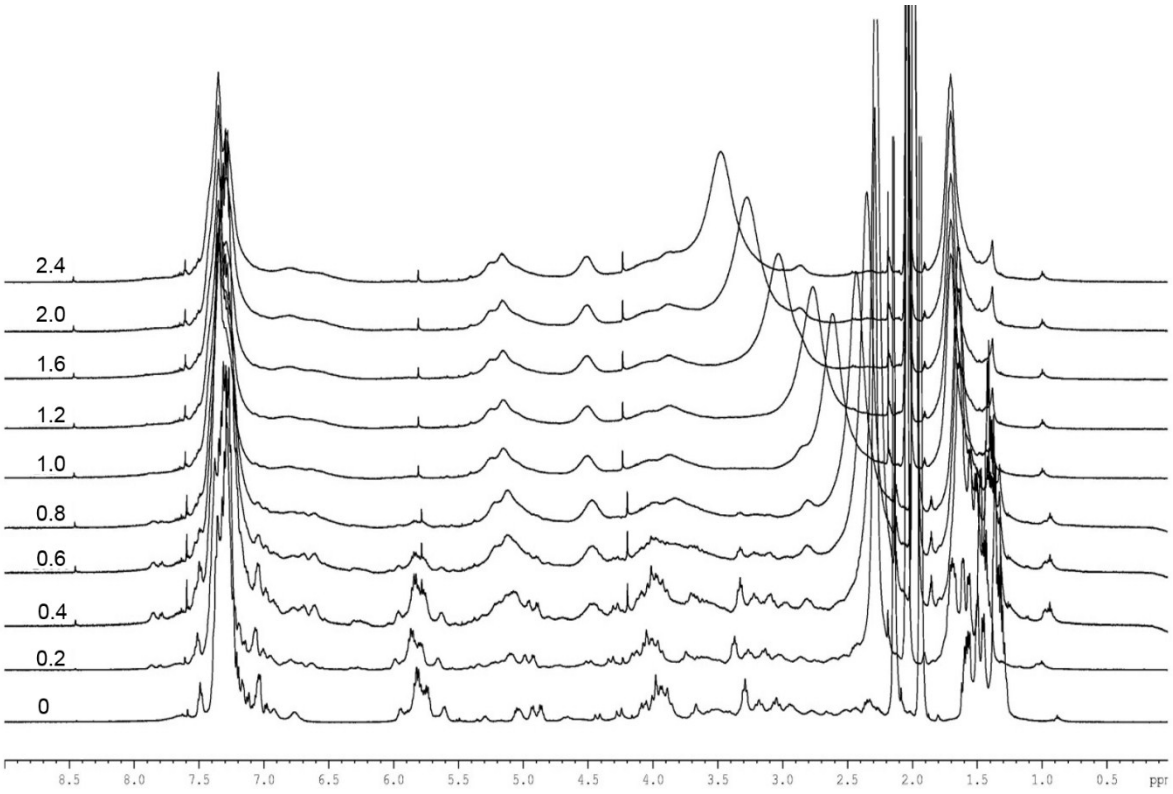

Fig.S19. Quantitative titration by ^{1}H NMR of $Mg(ClO_4)_2$ into peptoid **cP1** at the molar ratios (Mg^{2+}/**cP1**) indicated. All experiments were performed in CD_3CN at 293K using a peptoid concentration of 8 mM.

(Conformation A) Sr^{2+}cP1 (6 co-ordinate)

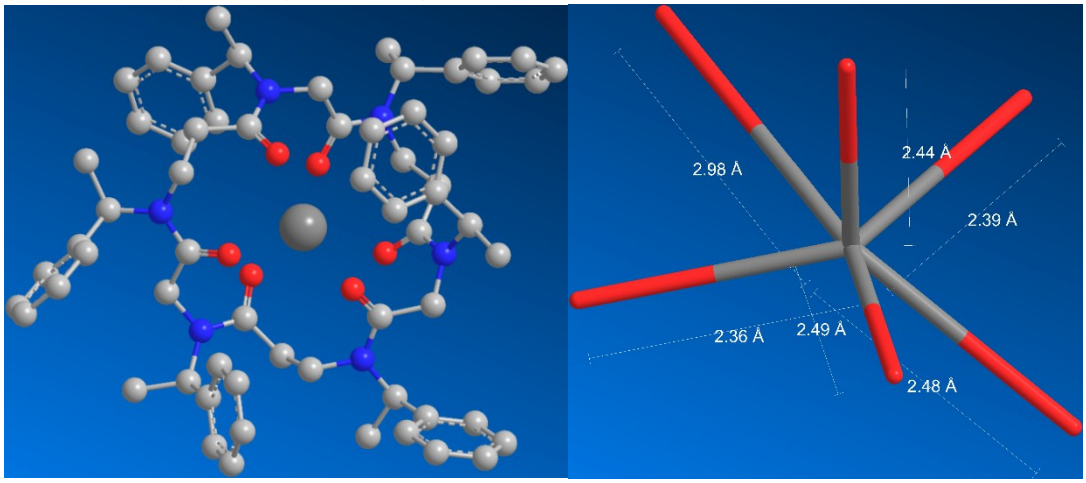

Mopac Interface: Heat of Formation = 211.41164 kJ/Mol
Mopac Interface: Total Energy = -11530.02188 eV

(Conformation B) Sr^{2+}cP1 (6 co-ordinate)

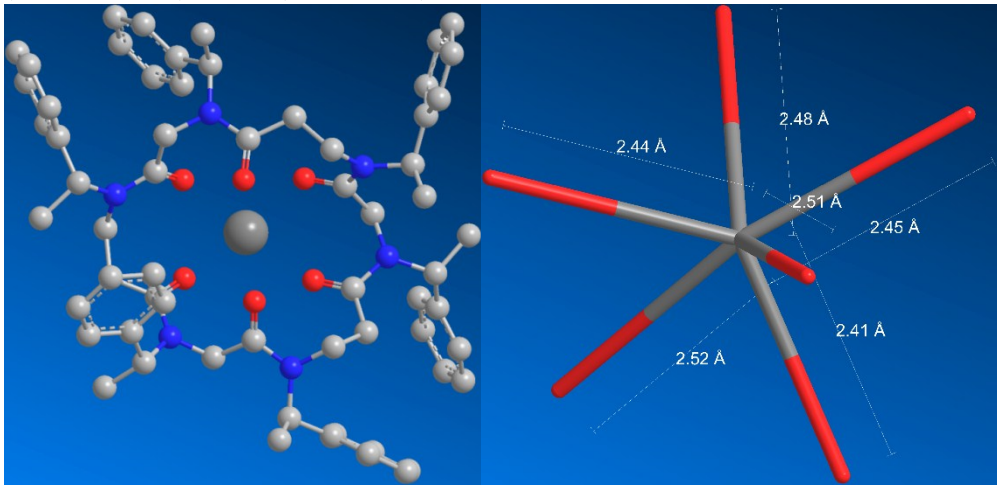

Mopac Interface: Heat of Formation = 223.97107 KJ/Mol
Mopac Interface: Total Energy = -11529.89867 eV

(Conformation C) Sr^{2+}cP1 (6 co-ordinate)

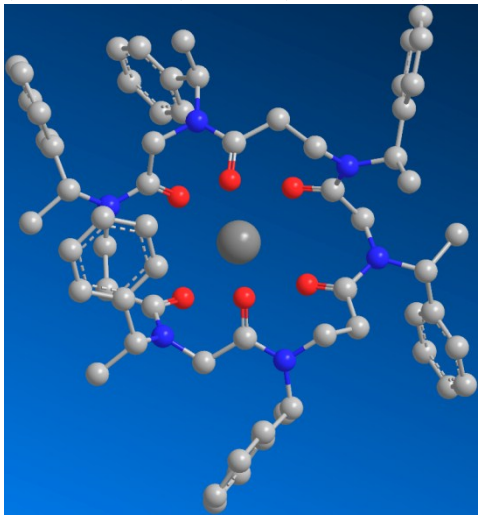

Mopac Interface: Heat of Formation = 218.93146 KJ/Mol
Mopac Interface: Total Energy = -11529.94510 eV

(Conformation D) Sr^{2+}cP1 (4 co-ordinate)

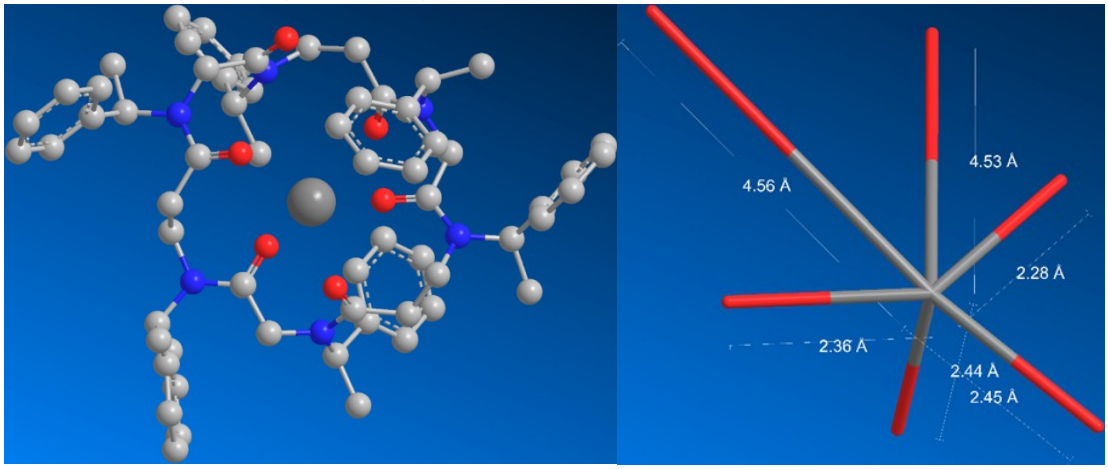

Mopac Interface: Heat of Formation = 274.73539 KJ/Mol
Mopac Interface: Total Energy = -11529.36399 eV

(Conformation E) Sr^{2+}cP1 (6 co-ordinate)

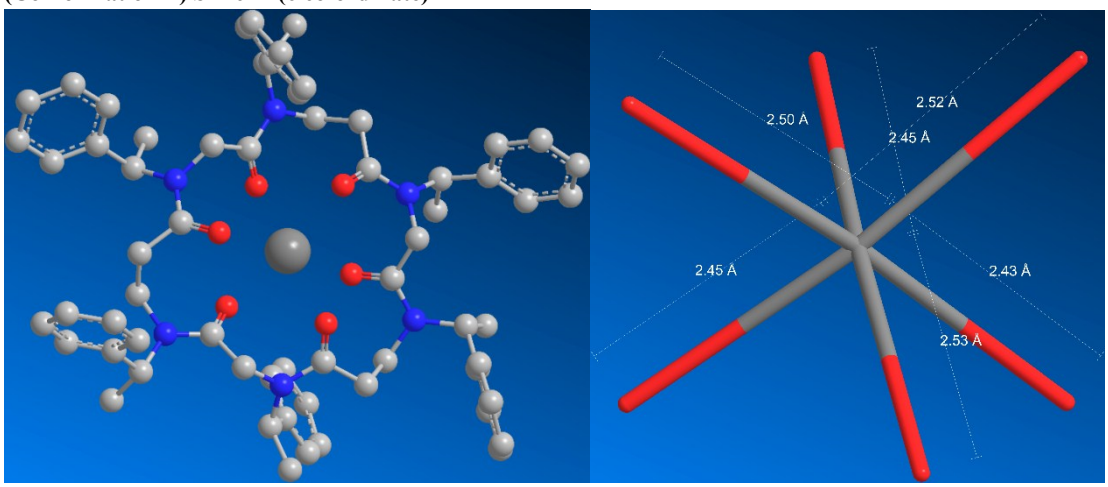

Mopac Interface: Heat of Formation = 191.76602 KJ/Mol
Mopac Interface: Total Energy = -11530.21659 eV

Conformer	Mopac Interface	
	Heat of Formation (kJ/Mol)	Total Energy (eV)
(A) Sr^{2+}cP1 (6 co-ordinate)	211.41164	-11530.02188
(B) Sr^{2+}cP1 (6 co-ordinate)	223.97107	-11529.89867
(C) Sr^{2+}cP1 (6 co-ordinate)	218.93146	-11529.94510
(D) Sr^{2+}cP1 (4 co-ordinate)	274.73539	-11529.36399
(E) Sr^{2+}cP1 (6 co-ordinate)	191.76602	-11530.21659

Fig.SI20. Representative minimum energy conformers with bond lengths for the C=O Sr^{2+} coordination for Sr^{2+}**cP1** in the gas phase.

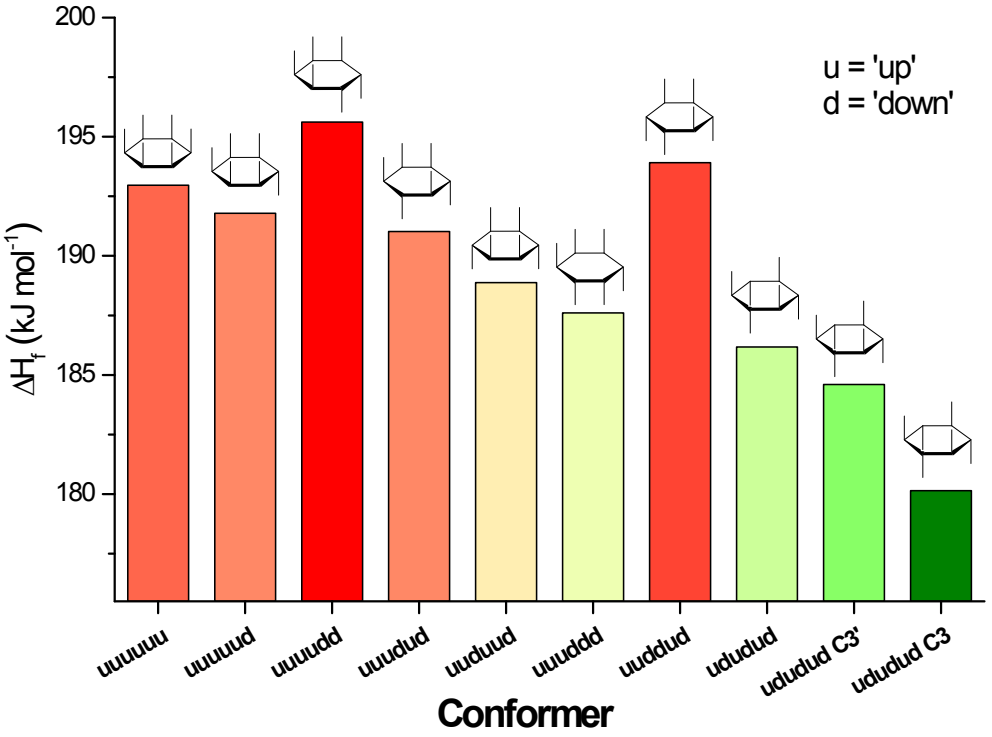

Fig.SI21. Heats of formation for the minimum energy conformers for the 6-coordinate Sr^{2+}**cP1** in the gas phase. The structures illustrated show the starting conformational arrangement of the ethylphenyl substituents relative to the plane of the ring.